- Technical Paper -

SEISMIC BEHAVIOR OF DRIFT-HARDENING PRECAST CONCRETE WALLS REINFORCED WITH SBPDN REBARS

Jiayu Che[*1], Chi Zhang[*1], Takashi Takeuchi[*2] and Yuping Sun[*3]

ABSTRACT

Four precast concrete walls whose edge zones were reinforced with ultra-high strength SBPDN bars were fabricated and tested under cyclic lateral loading and constant axial compression to investigate seismic behavior of the precast concrete walls and to clarify the necessary embedment length of the SBPDN bars into the foundation beams. The test results have indicated that embedment length of twenty times of SBPDN diameter could ensure the precast walls sufficient drift-hardening capability up to at least 2.0% drift ratio, and that the larger the shear span ratio, the larger the peak drift ratio.

Keywords: Precast concrete wall, shear span ratio, axial load ratio, embedment length, SBPDN bar

1. INTRODUCTION

Concrete shear walls have been widely used in residential buildings in earthquake-prone areas because of their large lateral stiffness and high lateral resistance [1,2]. During the last several decades, numerous analytical and experimental studies on seismic behavior of ductile concrete shear walls have been conducted [2-5]. The previous studies as well as the experience of recent catastrophic earthquakes have demonstrated that reasonably designed structural concrete walls can make mid-rise and high-rise reinforced concrete buildings have good lateral stability and resistance to displacement ductility under design base earthquakes. Many countries have also modified their design codes based on the results of analysis and experimentation.

Although conventional rectangular concrete walls have great horizontal load resistance, they are prone to concentrated severe damage at the end regions when subjected to earthquakes with greater intensity than anticipated, making them difficult to be repaired. In Japan, where dumbbell-shaped walls rather than rectangular walls have been adopted in building structures for over the past half a century, the revision of the design standard for concrete structures [6], allows rectangular shear walls without boundary columns to be designed as load-bearing elements in buildings.

Compared with the dumbbell-shaped walls, the rectangular walls have lower flexural capacity due to the lack of being restrained by boundary columns. To compensate for the low lateral resistance of rectangular concrete walls and reduce their residual deformation, Sun and his colleagues have proposed using ultra-high strength SBPDN rebars as longitudinal bars placed within the edge zones of wall panel, and experimentally verified that the proposed rectangular concrete walls could exhibit high drift-hardening capability that means the ability to increase its lateral resistance along with drift ratio, small residual deformation, and high repairability [7-9].

From the viewpoint of construction efficiency and quality, the authors have also investigated the feasibility

Table 1　Primary experimental parameters and main test results

Specimen	f_c' (MPa)	f_g' (MPa)	t (mm)	D (mm)	h (mm)	a/D	n	Concentrated SBPDN rebars	Longitudinal rebars		Transverse rebars		Sheath tube	
									ρ_{wy} (%)	Type	ρ_{wh} (%)	Type	Depth of Embedment (mm)	Diameter (mm)
WP15-20d-075	45.6	65.8	150	600	900	1.5	0.075	8-U12.6	0.35	10-D6	0.65	D6@65	310	45
WP15-25d-150	43.7	65.1					0.15						375	
WP20-20d-075	45.1	62.8			1200	2.0	0.075						310	
WP20-25d-150	44.5	50.1					0.15						375	

f_c'：concrete cylinder strength;　f_g'：grout cylinder strength;　h：clear height of wall panel;　a/D：shear span ratio;
n：axial load ratio（$= N/tDf_c$，N：axial force）;　ρ_{wy}: longitudinal reinforcement ratio ;　ρ_{wh}: transverse reinforcement ratio;

*1　Ph.D. Student, Graduate School of Engineering, Kobe University, JCI Student Member
*2　Associate Prof., Graduate School of Engineering, Kobe University, JCI Member
*3　Prof., Graduate School of Engineering, Kobe University, JCI Member

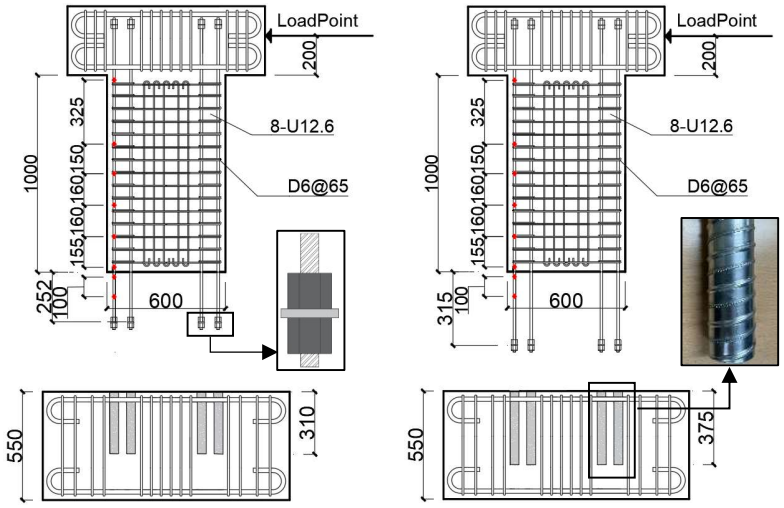

(a) WP20-20d-075 (b) WP20-25d-150

Fig.1 Reinforcement details of test shear walls (Unit: mm)

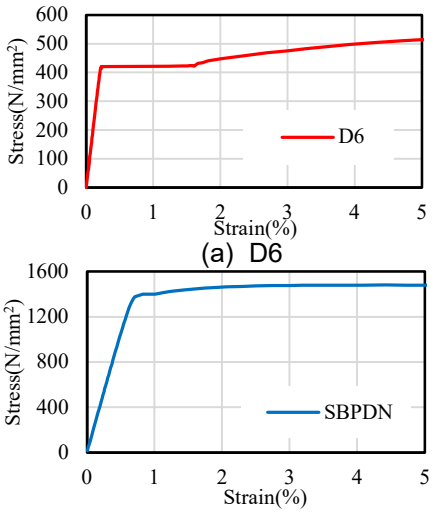

(a) D6 (b) SBPDN

Fig.2 Stress-strain relationships of the steels used

Table 2 Mechanical properties of the steels

Types		E_s (kN/mm²)	f_y (N/mm²)	ε_y (×0.01)	f_u (N/mm²)
D6	SD295A	196	400	0.23	530
U12.6	SBPDN 1275/1420	212	1399*	0.86*	1480

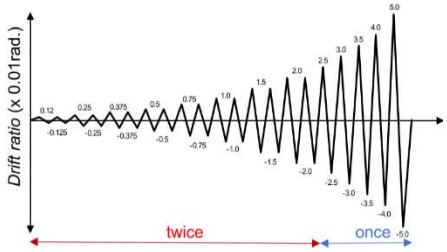

Fig.3 Loading program

of prefabrication of the drift-hardening concrete walls. With the embedment length of SBPDN bars, axial load ratio, and shear span ratio as main experimental variables, Che et al have experimentally study the effects of these factors on seismic behavior of precast walls reinforced by SBPDN bars bundled within one sheath duct and concluded that the embedment length of 35d (d is the nominal diameter of SBPDN bar) could ensure the precast walls the same drift-hardening capability as the cast-in-place walls [10,11].

To further optimize construction process, this paper investigates the effect of embedment length on the seismic performance of precast concrete walls reinforced by SBPDN bars, each of which was separately anchored into respective sheath duct and find the necessary embedment length for SBPDN bar.

2. Experimental program and material

2.1 Material properties and design of specimens

Table 1 and Fig. 1 respectively show outline of the specimens and their reinforcement details. Ready-mixed concrete with design strength of 30 MPa was used to fabricate specimens. Non-shrink grouting grout (PREU-LOX) was used for the post-assembly casting. Three ϕ100mm concrete cylinders and three ϕ50mm grout cylinders of each specimen were cured under the same conditions. The average values of the measured compressive strength are listed in Table .1. Table. 2 and Fig. 2 showed mechanical properties and stress-strain relationship of utilized rebars. The specimens are about 1/3 scale with wall thickness and depth of 150 mm and 600 mm, respectively, while the wall heights are 700 mm

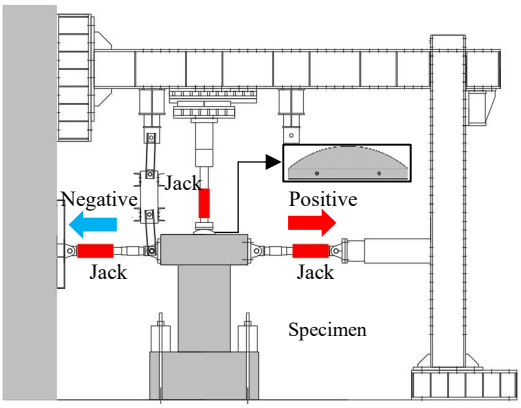

Fig.4 Schematic view of test setup

and 1000mm to give shear span ratios of 1.5 and 2.0, for WP15 series and WP20 series respectively. Both longitudinal and transverse bars of wall panel consisted of D6 deformed bars with spacing of 65 mm.

In the names of specimens (e.g. WP20-20d-075), the first combination of letters and numbers (WP20) means wall panel with shear span ratio of 2.0, the second one (20d) represents embedment length of 20d for SBPDN bar, and the third and last one (075) expresses axial load ratio of 0.075.

The wall panel was cast as the upper part of the specimen together with the upper loading beam, and the lower loading beam was cast separately. Seven days after concrete placement, as shown in Fig. 1, the upper wall panel was lifted by a crane, and each SBPDN rebar with a washer and nuts preset at its lower end (see Fig. 1) was inserted into sheath duct embedded in the lower loading

(a) WP15-20d-075

(b) WP15-25d-150

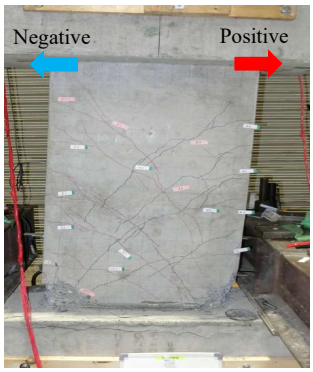

(c) WP20-20d-075

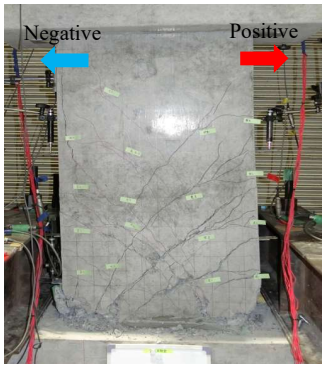

(d) WP20-25d-150

Fig.5 Ultimate states of specimens after testing

(a) WP15-20d-075 (after testing)

(b) WP20-20d-075 (at R=-4.0%)

Fig.6 Damage observed at the wall toes

beam, then grouted to integrate them. The boundary surfaces between the wall panel and the lower loading beam were roughened with bubble wrap, and the joint portion of 6 mm in thickness was also filled with grout. The #1000-series sheath ducts which were made of thin iron sheets (see Fig. 1) with spiral grooves on their surface were used to house SBPDN bars.

2.2 Test setup and loading procedures

Fig. 4 shows the loading apparatus. A 1000 kN hydraulic jack was used to apply the prescribed axial load, and two 500 kN jacks were used to repeatedly apply lateral force. Between the upper loading beam and the 1000 kN jack, a cylindrical steel seat was placed to keep the center of rotation on the action line of the cyclic lateral force. The lateral loading was controlled by drift ratio (R), which is defined as the ratio of the lateral displacement (Δ) at the loading point of lateral force to the shear span of walls. Fig. 3 shows the designed loading protocol. As shown in Fig. 3, the lateral load cycles were applied for two completely reversed cycles at each drift ratio of R=0.25%, 0.375%, 0.5%, 0.75%, 1%, 1.5%, 2%, and one complete cycle each at the drift levels of R=2.5%, 3%, 3.5%, and 4%. The loading would be terminated either when the specimen lost its gravity sustaining capacity or when the lateral load fell below 85% of the maximum lateral force. Before applying the lateral force following the designed protocol, to confirm the stage of occurrence of the first flexure crack and shear crack, the lateral load was controlled by force at an interval of 10 kN before R reached 0.125%.

3. Experimental results and discussion

3.1 Cracks and damage of specimens

Fig. 5 shows overall ultimate state of each specimen observed after the testing, and Fig. 6 displays examples of the damage observed near the wall toes. Fig. 7 shows the measured lateral force (V) versus drift ratio (R) relationships of all specimens.

For specimen WP15-20d-075, flexural crack was firstly observed at drift ratio of 0.125% in both positive and negative direction. The flexural cracks began to propagate in diagonal direction at R= 0.25%. Longitudinal cracks appeared on the surface of compressed concrete around R = 0.75% in the negative direction and around R = 1% in the positive direction. Spalling-off of concrete was observed when the drift ratio approached 1.5%. From then, the damage of compressed concrete became more severe along with the drift ratio. The lateral resistance continued increasing up to the drift ratio of 3% as shown in Fig. 7. During the loading toward 3.5%, the shear crack became wider and the lateral resistance degraded. However, as shown in Fig. 6(a), where the positions of sheath ducts are marked with red dashed circles, the sheath ducts were completely intact, which implies that embedment depth of 20d is sufficient to prevent the SBPDN bar from premature pulling-out.

For specimen WP15-25d-150, the first flexural cracks occurred at R= 0.125%. Shear crack was observed at R= 0.25%. Longitudinal crack was observed on the compression side of the wall toe at the drift ratio of 1.0 %. This specimen developed its maximum lateral resistance at the drift ratio of 2.0%. From R=2.5%, spalling-off of compressed concrete became more severe,

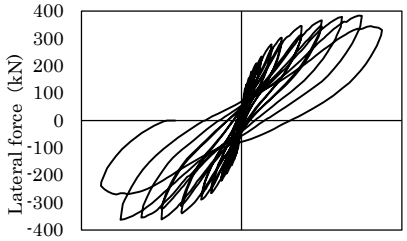

(a) WP15-20d-075

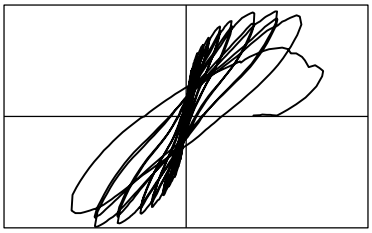

(b) WP15-25d-150

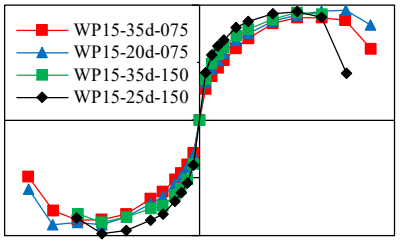

(a) a/D=1.5

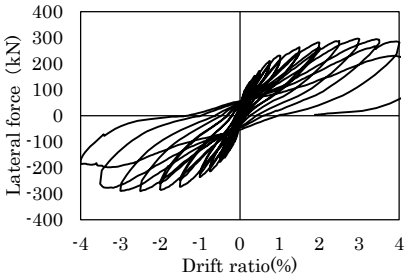

(c) WP20-20d-075

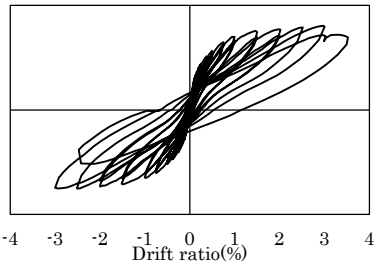

(d) WP20-25d-150

Fig.7 Measured lateral load-drift ratio relationships

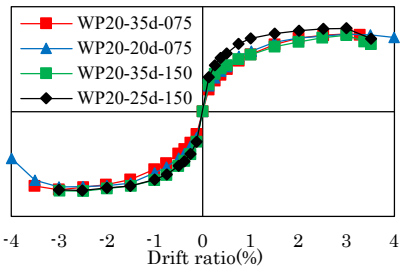

(b) a/D=2.0

Fig.8 Skeleton curves

which caused the degradation of lateral resistance. During pushing toward drift ratio of 3.0%, the shear crack widened and resulted in abrupt decrease of lateral resistance.

As for specimen WP20-20d-075 with shear span ratio of 2.0, the flexural and shear cracks were observed at the drift ratios of 0.125% and 0.25%, respectively. Spalling-off of concrete was observed at the drift ratio of around 1.5%. The specimen reached its maximum lateral resistance at R= 3.0%, but still maintained over 90% of the maximum loading till drift ratio of 4.0% while grout and concrete at the compressed side crushed more severely. During loading toward R= -4.0%, horizontal cracks appeared near and top face of the loading stub and the sheath ducts began to be pulled-out (see Fig.6(b)), resulting in the significant decrease of lateral resistance.

As the other three specimens, for specimen WP20-25d-150, the first flexural and shear crack were observed at the drift ratio of 0.125% and 0.25%, respectively. Spalling-off of concrete occurred at drift ratio of 1.5%. The maximum lateral resistance was reached at the drift ratio of 3.0 % in the positive direction and of -2.5% in the negative direction, respectively. The lateral resistance began to decrease during the loading cycle of R=3.5% due to significant crushing of compressed concrete. Premature pulling-out of sheath ducts was not observed.

The above observations indicate that the higher the axial load level, the smaller the drift-hardening drift ratio, and that the larger the shear span, the larger the drift-hardening drift ratio.

3.2 Effect of embedment length of SBPDN bars

The skeleton curves of all specimens are depicted in Fig. 8 according to shear span ratio. The skeleton curves are obtained by connecting the peak load points at each drift ratio. For comparison and investigation of effect of the embedment length of SBPDN bar, the skeleton curves of specimens with embedment length of

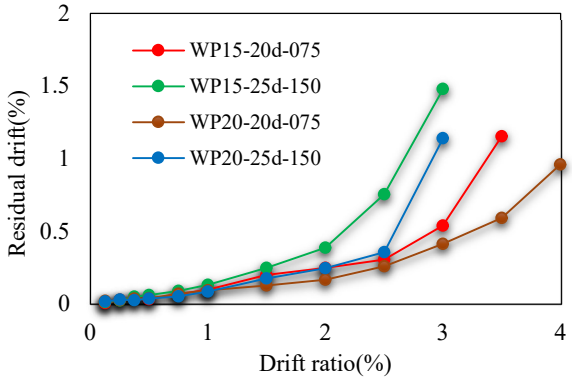

Fig.9 Residual drift ratios

35d reported by the authors [10] are also shown in Fig. 8. It can be seen from Fig. 8 that there is no significant discrepancy between the specimens with the identical experimental conditions, which implies that the embedment length of 20d is enough to prevent SBPDN bar in the proposed precast drift-hardening concrete walls from premature pulling-out and ensure sufficient drift-hardening capability to the walls.

3.3 Residual drift ratios

Fig. 9 shows the experimental results of the residual drift ratios for all specimen. The residual drift ratios represent the average of those measured in positive and negative direction. The residual drift ratios of all specimens were controlled below 0.5% till the drift ratio of 2.0% regardless of the shear span ratio and axial load ratio. From R=2.0% on, the higher the axial load ratio and the larger the shear span ratio, the larger the residual drift ratio became. For the specimens under axial load ratio of 0.075, their residual drift ratios after unloading from R=3.0% were still kept under 0.5%.

3.4 Measured strains of SBPDN bars

The measured axial strains of SBPDN bars for all

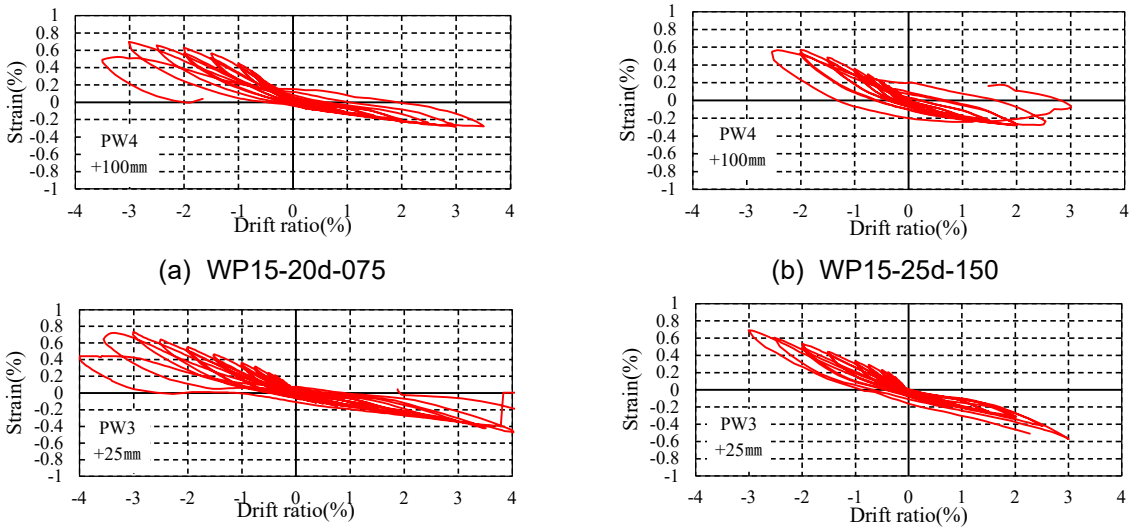

(a) WP15-20d-075 (b) WP15-25d-150

(c) WP20-20d-075 (d) WP20-25d-150

Fig. 10 Measured strains of SBPDN bars

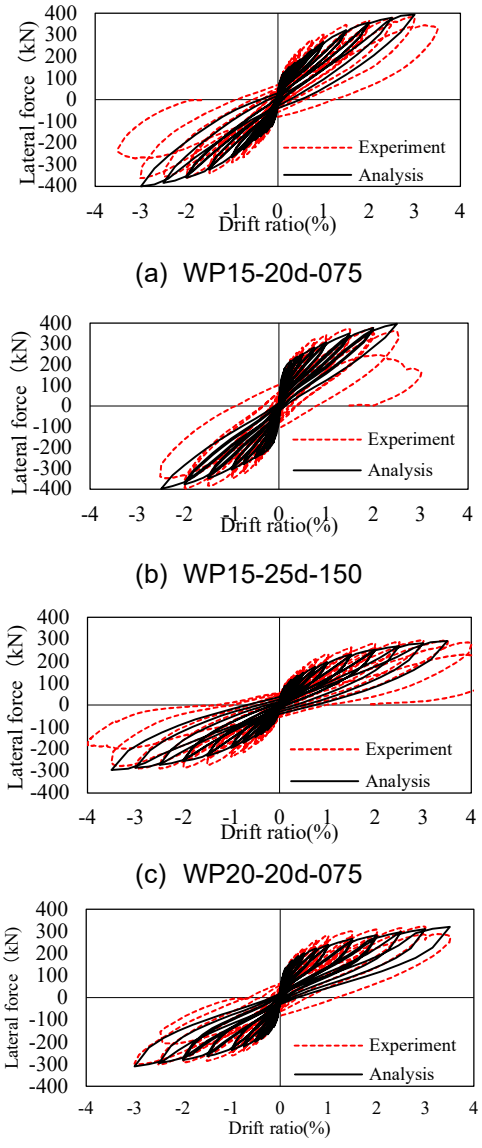

(a) WP15-20d-075

(b) WP15-25d-150

(c) WP20-20d-075

(d) WP20-25d-150

Fig.11 Comparisons of the experimental and the calculated hysteresis loops

specimens are shown in Fig.10. The strains shown in Fig.10 represent those measured by the strain gages located on the initial tensile edge of the wall section and at the section of 25mm away from the wall toes for specimens WP20-20d-075 and WP20-25d-150. The strains of specimens WP15-20d-075 and WP15-25d-150 were those measured at the section 100mm away from the wall toe because the data at 25mm-section could not experimentally be obtained due to disconnection of the gage wires there. It was apparent that the axial strains of SBPDN bars revealed similar behaviors to the lateral force (see Fig. 7) and did not reach its yield strain (0.84%) till the end of loading, which accounted for the stable increase in the steel stress.

This observation implies that SBPDN bars could provide increasing lateral force up to large drift. This increment by SBPDN bars can compensate for the loss in lateral resistance caused by significant spalling of the concrete cover as well as the so-called P-Delta effect, enabling the overall lateral resistance of the walls to stably increase along with the drift ratio and ensuring the proposed precast concrete walls sufficient drift-hardening capability.

4. Analysis of cyclic performance of the walls

4.1 Description of analytical method

In this study, to evaluate seismic performance of the proposed precast concrete walls reinforced by ultra-high strength SBPDN bars, the finite springs method (FSM) refined by Kitajima et al [13] will be adopted. The FSM is utilized to take into account the effects of slippage of SBPDN bars on overall seismic performance and provide more accurate prediction of the precast concrete walls.

In utilizing the FSM method, the following basic assumptions are made: 1) concrete does not resist tensile stress, 2) the concrete plane remains plane after bending, 3) the constitutive model of concrete proposed by Sakino and Sun was used in this analysis, 4) the bond stress-slip relationship of the SBPDN bar follows the model proposed by Funato et al [14], and the modified

Menegotto-Pinto model is utilized as the constitutive model of SBPDN bar, 5) the lengths of plastic end region of the walls with shear span ratio of 1.5 and 2.0 will be 0.65D and 0.75D (D is the depth of the wall section), respectively[12], 6) strain and stress of the longitudinal bars are uniformly distributed in the plastic hinge region, 7) the SBPDN bars are completely fixed at both ends. The seventh assumption represents the end boundary condition of SBPDN bars and is necessary when using FSM to predict the effect of slippage.

4.2 Comparisons of test and calculated V-R curves

To verify the reliability and accuracy of the presented analytical method for evaluating the seismic performance of the precast concrete walls, the results calculated by the analytical method are compared with the experimental ones in Fig. 11 in the form of cyclic V-R relationship. It can be seen from Fig. 11 that the calculated hysteresis loops can trace the experimental results up to peak drift ratio with very satisfactory accuracy. After the peak point, the difference between the calculated results and the measured ones becomes large because the analytical method ignores the influence of the shear failure at large drift, which needs further study in the future.

5. Conclusions

This paper is intended to investigate the influence of the embedment depth of SBPDN bars on the seismic performance of drift-hardening precast concrete walls. Four specimens were fabricated and tested under combined reversed lateral loading and constant axial compression with shear span ratio and embedment length of SBPDN bars and axial load ratio as primary experimental variables. Based on the experimental works described in this paper, the following conclusions can be drawn:

(1) When fixed at both ends by washer and nuts, an embedment length of 20d of SBPDN bars could ensure sufficient drift-hardening capability to the precast rectangular concrete walls. Within the testing range of this study, the axial load ratio and embedment length do not influence each other if the embedment length is longer or equal to 20d.

(2) For the walls under axial load ratio of 0.075, the proposed precast concrete walls with shear span ratios of 1.5 and 2.0 exhibited drift-hardening behavior up to drift ratios of 2.5% and 3.5%, respectively. For the precast concrete walls under axial load ratio of 0.15, the walls with shear span ratios of 1.5 and 2.0 showed drift-hardening behavior up to drift ratios of 2.0% and 3.0%.

(3) The analytical method presented in this paper could predict the experimental hysteresis response of all specimens up to the drift-hardening drift ratio with very satisfactory accuracy. To accurately trace the post-peak behavior of the drift-hardening precast walls, further study is needed to account for the effect of shear failure.

ACKNOWLEDGEMENTS

This study was financially supported by JSPS KAKENHI Grant Number 19H02289. SBPDN rebars were provided by Neturen Co. Ltd. Assistance to the experiment described in this paper by Mr. Kanao, technical staff of Kobe University is greatly appreciated.

REFERENCES

[1] Fintel M. (1995): “Performance of buildings with shear walls in earthquakes of the last thirty years, PCI, Vol.40, pp.62-80.

[2] Holden T, Restrepo J, Mander JB. (2003): “Seismic performance of precast reinforced and prestressed concrete walls”. J Struct ASCE, Vol.129, pp.286–296.

[3] Sezen H, Whittaker AS, Elwood KJ, Mosalam KM., (2003): “Performance of reinforced concrete buildings during the August 17, 1999 Kocaeli, Turkey earthquake, and seismic design and construction practice in Turkey”. Eng Struct, Vol.25, pp.103–114.

[4] Wyllie LA Jr, Filson JR. (1989): “Armenia earthquake reconnaissance report." Earthq Spectra Publication Special Supplement, No. 89.01.

[5] Kuramoto H. (2006): “Seismic design codes for buildings in Japan.” J Disaster Res. Vol.1, pp.341–356.

[6] Architectural Institute of Japan (2010): “AIJ Standard for Structural Calculation of Reinforcement Concrete Structure”, pp. 274-275.

[7] Y Sun. et al. (2013): “Fundamental study of seismic performance of resilient concrete columns”. Proceedings of the JCI, 35(2), pp. 1501-1506.

[8] Tani M. et al. (2009) “Experimental study of resilience of concrete columns made of high-strength materials”. Proceedings of the JCI, 31(2), pp. 565-570.

[9] Y Sun. et al. (2006): “Analytical Study of Cyclic Response of Concrete Members Made of High-Strength Materials”. The Eighth U.S. National Conference on Earthquake Engineering, Paper No. 1581.

[10] J Che. et al. (2022): “Seismic Behavior and Bond Performance of Rectangular Precast Concrete Walls Reinforced with Ultra-high Strength Rebars”. Journal of Structural Engineering, Vol.68, pp. 87-96.

[11] J Che. et al. (2021) “Seismic performance of precast RC shear walls reinforced by SBPDN rebars”, Proceedings of the JCI, 43(2), pp. 169-174.

[12] C. Wei, Y. Sun, T. Takeuchi, T. Nakagawa: Seismic Behaviors and evaluation of reinforced concrete walls confined by SBPDN rebars, Proceedings of the JCI, 2021, 43(2), pp. 175-180.

[13] Kitajima H., Sun Y., Fukuhara T.(2006): Analytical Study of Cyclic Response of Concrete Members Made of High-Strength Materials,” Proceedings of the 8th U.S. NCEE, Paper No. 1581.

[14] Funato Y., Sun Y., Takeuchi T., and Cai G.(2012), “Modeling and Application of Bond Characteristic of High-strength Reinforcing Bar with Spiral Grooves,” Proceedings of the Japan Concrete Institute, V.34, No.2, pp.157-162